Volume fraction profile in channeled granular flows down an erodible incline

M. Y. Louge
Sibley School of Mechanical and Aerospace Engineering, Cornell University, Ithaca, NY 14853 USA
A. Valance, N. Taberlet, P. Richard & R. Delannay
Groupe Matière Condensée et Matériaux, UMR CNRS 6626, F-35042 Rennes cedex, France

We use a momentum balance to interpret numerical simulations of dense, steady, fully-developed inclined granular flows of spheres on an erodible base confined between flat frictional side walls. We observe an exponential profile of mean volume fraction in the direction perpendicular to the base and suggest a scaling for its characteristic length. We also predict volume fraction and mean velocity profiles in the ballistic region above the free surface.

1 INTRODUCTION

Taberlet et al. (2003) recently reported experiments in which grains poured in a channel confined by flat, frictional side walls establish a rectilinear flowing layer of fixed height above a deep static heap. Because the flow inclination is considerably larger than the angle of repose, they referred to this phenomenon as a "Super Stable Heap" (SSH). In a companion paper appearing elsewhere in these proceedings, Taberlet et al. (2005) describe numerical simulations revealing details that the physical experiments could not record. Beside reproducing already identified features of the phenomenon, the simulations prove that the mobilized layer is steady and fully-developed (SFD). In this article, we interpret the new results with a momentum balance that is informed by the simulations. We also outline a theory for the dilute surface layer where grains undergo ballistic trajectories with rare collisions. We begin with a summary of observations.

2 OBSERVATIONS

Figure 1 shows simulation profiles for the volume fraction ν and the streamwise velocity $u_x/\sqrt{gd}$ made dimensionless with the gravitational acceleration g and the spherical grain diameter d from Taberlet et al. (2005). These variables are averaged in the direction z perpendicular to side walls separated by a width W. Their profiles are shown along the downward direction s perpendicular to the free surface. In SFD flow, all flow variables are independent of the streamwise direction x, and the free surface and erodible base form a common angle α with the horizontal. In the simulations, the Coulomb friction coefficient of a sphere with another sphere or with the side walls is μ.

We locate the free surface where the velocity pro-

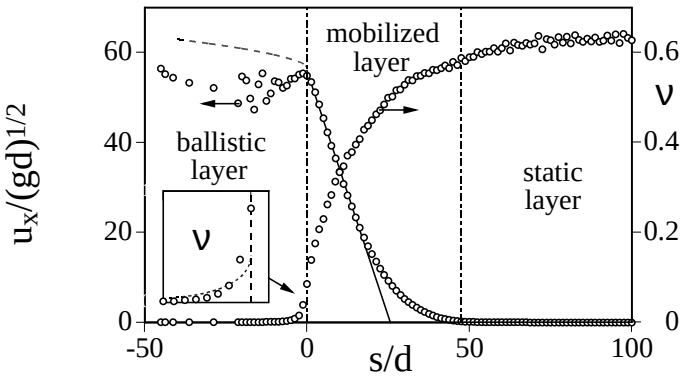

Figure 1. Profiles of dimensionless mean velocity and volume fraction. Conditions are $\mu = 0.8$, $W/d = 20$, $\alpha = 45°$. We find $\nu_s \sim 0.62$, $\nu_0 \sim 0.08$ and $s_m/d \sim 48$. Flow regions are separated by vertical dashed lines. The slanted line determines the intercept $h/d \sim 26$. The dashed curve is the model of Eq. 23 for $s < 0$. The insert shows a detail of ν near the free surface, with the superimposed prediction of Eq. 19.

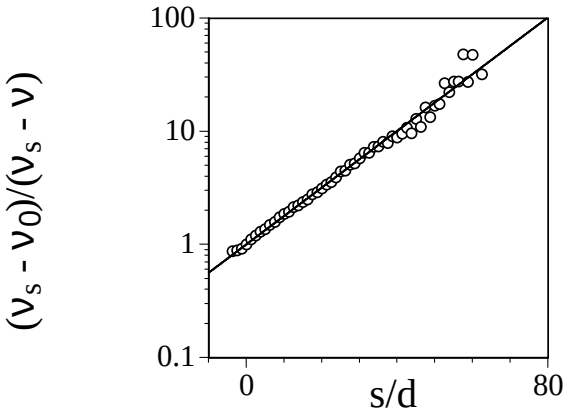

Figure 2. $-\log_{10}[(\nu_s - \nu_0)/(\nu_s - \nu)]$ *vs.* s/d with conditions of Fig. 1. We find $\ell/d \sim 17$.

file exhibits a sharp change in slope. We place the origin of our coordinate system (x, s, z) there and on the centerline of the channel. Above the free surface, grains are thrown upwards in ballistic trajectories to a dilute region experiencing rare collisions. In this ballistic layer where $s < 0$, $u_x/\sqrt{gd}$ varies little and ν decreases away from the free surface with $d^2\nu/ds^2 > 0$.

Below, the mean volume fraction rises exponentially from the volume fraction ν_0 at the free surface to the random loose packing $\nu_s \approx 0.62$ on a characteristic length scale ℓ

$$\nu = \nu_0 + (\nu_s - \nu_0)[1 - \exp(-s/\ell)] \tag{1}$$

Here, $d^2\nu/ds^2 < 0$. In this region, the profile of $u_x/\sqrt{gd}$ also resembles an exponential decay along s with characteristic length h (Komatsu et al. 2001), which provides a convenient measure of depth of the mobilized layer in physical experiments (Taberlet et al. 2003). At $s = s_m$ where most grains are no longer mobilized, we expect that the volume fraction is $\nu = \nu_m \approx 0.59$ i.e, just above the glass transition for hard spheres $\nu_{glass} \sim 0.58$. This value of ν_m is also the largest volume fraction that Silbert et al. (2001) observed in their own simulations.

Taberlet et al. (2003) invoke a force balance assuming constant volume fraction and constant wall friction to explain their empirical observation of

$$\tan\alpha = \mu_m + \mu_w(h/W). \tag{2}$$

They then interpret μ_w as an effective friction coefficient at the side walls that accounts for rolling or sliding contacts. Thus, because such interactions produce a ratio of tangential to normal force no greater than μ, these authors expect $\mu_w \leq \mu$. Simulations confirm the trends predicted by Eq. 2 (Taberlet et al. 2005). Next, we refine the force balance by incorporating new information on the volume fraction profile.

3 MOMENTUM EQUATIONS

We consider the regime in which side walls affect the flow. Taberlet, et al. (2005) suggest that this is where $\xi \equiv (h\mu_w)/(W\mu_m) \geq 1$. The momentum balances for this two-dimensional SFD flow are

$$\frac{\partial\tau_{xs}}{\partial s} + \frac{\partial\tau_{xz}}{\partial z} = -\rho_s g\nu\sin\alpha \tag{3}$$

along x and, assuming that the s-component of the contact forces between particles and side walls are negligible (no "Janssen effect"),

$$\frac{\partial\tau_{ss}}{\partial s} = +\rho_s g\nu\cos\alpha \tag{4}$$

along s. In these Eqs., τ_{ij} is the stress tensor along i on surfaces of normal j, and ρ_s is the material density of the grains. We invoke the following assumptions: the normal stress is isotropic, $\tau_{ss} = \tau_{zz}$; $\nu = \nu(s)$; the flow surface is flat and perpendicular to s; τ_{xs} depends only on s; and side walls are identical. We define the ratio $\mu_\tau(s)$ of shear to normal stress at the walls such that $\tau_{xz} \equiv \mp\mu_\tau(s)\tau_{zz} \equiv \mp\mu_\tau(s)\tau_{ss}$ at $z = \pm W/2$.

Integrating Eq. 3 along z and Eq. 4 along s yields

$$\frac{d\tau_{xs}}{ds} = -\rho_s g\nu\sin\alpha + 2\mu_\tau\frac{\tau_{ss}}{W} \tag{5}$$

and

$$\tau_{ss} = \rho_s g\cos\alpha\int_{-\infty}^{s}\nu d\theta. \tag{6}$$

Substituting in Eq. 5, integrating further along s, and dividing by Eq. 6, we find the effective friction on surfaces at constant s

$$\mu_{eff} \equiv -\frac{\tau_{xs}}{\tau_{ss}} = \tan\alpha - \frac{\sigma_\mu}{W}, \tag{7}$$

where we define the "friction depth" as

$$\sigma_\mu(s) \equiv 2\frac{\int_{-\infty}^{s}\mu_\tau(\zeta)d\zeta\int_{-\infty}^{\zeta}\nu d\theta}{\int_{-\infty}^{s}\nu d\theta}. \tag{8}$$

Comparing Eqs. 2 and 7, we identify

$$\mu_m \equiv \mu_{eff}(s = s_m) \tag{9}$$

and

$$h\mu_w \equiv \sigma_\mu(s = s_m). \tag{10}$$

We evaluate the integrals in Eq. 6 and 8 to estimate μ_w. To that end, we invoke further simplifying assumptions. First, because volume fractions are small in the rarefied ballistic layer, we ignore the contribution of $s \in]-\infty, 0]$ to these integrals. Second, we take the point of contact at the wall to be engaged in gross slip throughout the mobilized depth with constant $\mu_\tau(s) = \mu_\tau, \forall s \leq s_m$, from which we expect $\mu_\tau \leq \mu$. Third, we simplify Eq. 1 using $\nu_0 \ll \nu_s$. Accordingly,

$$\sigma_\mu \approx s\mu_\tau\left[\frac{1 - 2(\ell/s) + 2(\ell/s)^2(1 - e^{-s/\ell})}{1 - (\ell/s)(1 - e^{-s/\ell})}\right] \tag{11}$$

for $s \leq s_m$. Remarkably, σ_μ is nearly linear in s, and thus the effective friction decreases with distance from the free surface. Expanding Eq. 11 near $s/\ell \sim 0$,

$$\sigma_\mu = \frac{2}{3}\mu_\tau\, s\Big[1 + \frac{1}{12}\Big(\frac{s}{\ell}\Big) - \frac{1}{180}\Big(\frac{s}{\ell}\Big)^2 + O\Big(\frac{s}{\ell}\Big)^3\Big] \tag{12}$$

with relative error from Eq. 11 $< 0.5\%$ at $s/\ell \leq 5$. Thus in general, σ_μ depends weakly on ℓ, ν_s or ν_0. Combining Eqs. 10 and 11 with $\nu = \nu_m$ at $s = s_m$,

$$\frac{h\mu_w}{\ell} = \mu_\tau r_m\left[\frac{1 - (2/r_m) + (2/r_m^2)(\nu_m/\nu_s)}{1 - (\nu_m/\nu_s)(1/r_m)}\right], \tag{13}$$

where $r_m \equiv \ln\nu_s - \ln(\nu_s - \nu_m)$. Thus, comparing the measured value of $h\mu_w/\ell$ with the predictions of

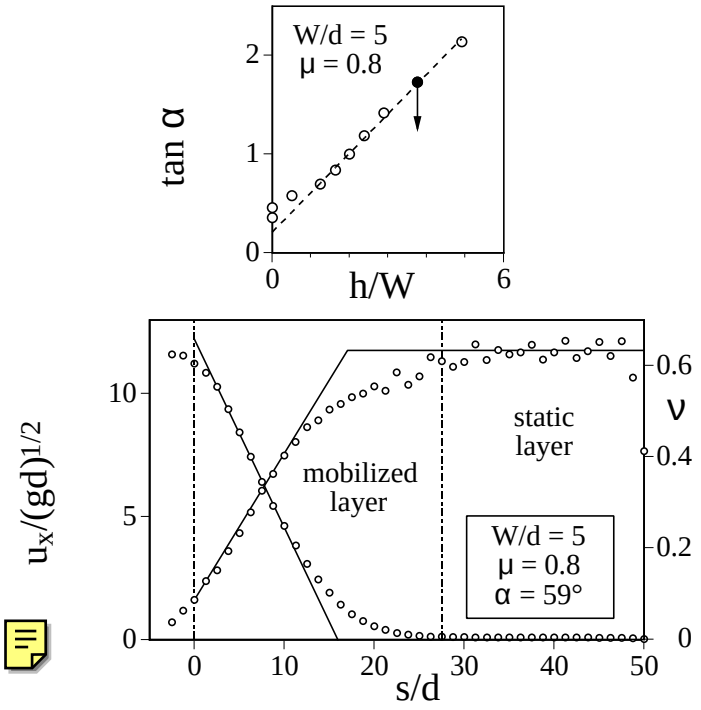

Figure 3. Bottom: Profiles of $u_x/\sqrt{gd}$ and ν for the conditions shown. We find $\nu_s \sim 0.63$, $\nu_0 \sim 0.09$, $s_m/d \sim 28$, $h/d \sim 16$, and $\ell/d \sim 15$. Lines and symbols, see Fig. 1. Top: $\tan\alpha$ *vs.* h/W. The filled circle refers to conditions of the bottom graph. We find $\mu_w \sim 0.4$ and $\mu_m \sim 0.21$.

Eq. 13 lets us relate μ_τ to μ. We expect $\mu_\tau \sim \mu$ for $W/d \gg 5$. However, we find sharp reductions in μ_τ when $W/d \leq 5$ (Taberlet et al. 2003). For example, we find $\mu_\tau \sim 0.18 \ll \mu$ with $W/d = 5$ (Fig. 3), which may betray the presence of rolling contacts at the side walls, or fluctuations in the direction of the contact velocity leading to a smaller projection along x of the average friction force.

We now discuss the origin of the intercept μ_m in Eq. 2. To that end, we first refer to experiments (Pouliquen 1999) and simulations (Silbert et al. 2001) for inclined flows on a bumpy base without side walls. Those SFD flows only exist above a minimum inclination $\tan\alpha_{min}$, which Louge (2003) calculated using a SFD energy balance of fluctuation energy in the core,

$$-\nabla \cdot q + \tau : \nabla u - \gamma = 0, \qquad (14)$$

where the gradient of the fluctuation energy flux q is negligible compared with the working of the shear stress τ through the velocity gradient ∇u or with the volumetric dissipation rate of fluctuation energy γ. Louge (2003) then expressed $\tan\alpha_{min}$ in terms of the internal friction μ_E of the granular assembly and coefficients of the dense kinetic theory that appear in the granular viscosity, $a_1 = 8(1+\pi/12)/(5\sqrt{5})$; in the volumetric dissipation rate of fluctuation energy, $a_3 = (12/\sqrt{\pi})(1-e^2)$, where e is a restitution coefficient; and in the equation of state, $a_4 = 4$,

$$\tan\alpha_{min} = \frac{\mu_E}{1 + \frac{\mu_E^2 a_4^2}{4 a_1 a_3}}. \qquad (15)$$

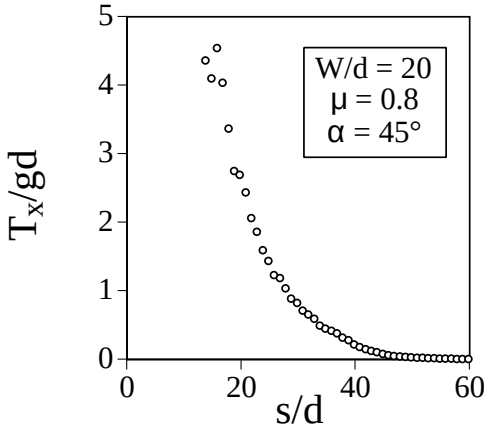

Figure 4. Granular temperature in the x-direction made dimensionless with $\sqrt{gd}$ *vs.* s/d for conditions of Fig. 1. Simulations of Taberlet, et al. (2005).

In the absence of side walls, the effective friction on planes parallel to the base is constant, $\mu_{eff} = \tan\alpha$ (Louge 2003). As Eq. 7 shows, the side walls modify the force balance by subtracting the friction depth σ_μ, which is roughly proportional to s. Thus, the side walls progressively reduce the effective friction from $\tan\alpha$ at the free surface down to the minimum value μ_m at which the flow begins to be mobilized. In this light, our conjecture is that μ_m is nearly given by Eq. 15,

$$\mu_m \sim \tan\alpha_{min}. \qquad (16)$$

However, μ_m may be somewhat smaller. The reason is that, while the term $-\nabla q \sim 0$ in the core of a flow without side walls, it is positive near $s \sim s_m$ in the SSH, $-\nabla q \propto d^2T/ds^2 > 0$, as Fig.4 suggests. Thus, the flux gradient term in Eq. 14 may contribute to grain mobilization at effective friction $< \tan\alpha_{min}$.

4 BALLISTIC LAYER

The steep inclination of SSH flows produces an agitated free surface from which spheres are ejected to a "ballistic" layer where they undergo mostly independent trajectories. Our objective is not to calculate boundary conditions for momentum and energy at the interface between a dense collisional flow and a region of freely flying grains (Jenkins & Hanes 1993). Here, we seek profiles of volume fraction and mean velocity in the ballistic layer. To model the latter, we ignore collisions and assume that the free surface has a number density $n_0 = 6\nu_0/\pi d^3$ with Maxwellian velocity distribution $\mathcal{M}_0$

$$\mathcal{M}_0 = \frac{n_0}{(2\pi T_0')^{3/2}} e^{-\frac{u_{0x}'^2}{2T_0'}} e^{-\frac{u_{0y}'^2}{2T_0'}} e^{-\frac{u_{0z}'^2}{2T_0'}} \qquad (17)$$

such that the average of a quantity ψ is

$$<\psi> = \frac{1}{n} \int\int\int \psi \mathcal{M}_0 du_{0x}' du_{0y}' du_{0z}' \qquad (18)$$

In these expressions, $x, y \equiv -s, z$ represent the three cartesian directions, and the subscript 0 indicates con-

ditions at the free surface. For convenience, we subtracted the mean velocity u_0 of the free surface to find $\mathcal{M}_0$. Our objective is to derive the corresponding distribution $\mathcal{M}$ at a distance η from that surface. To reach such distance, spheres must have $u_{0y} \geq \sqrt{2g\eta\cos\alpha}$. Primes in Eqs. 17 denote velocities and temperature made dimensionless with $\sqrt{g\eta\cos\alpha}$ and $g\eta\cos\alpha$, respectively. Thus, the number density at η is

$$n = \int_{\sqrt{2}}^{+\infty} \frac{n_0}{(2\pi T_0')^{1/2}} e^{-\frac{u_{0y}'^2}{2T_0'}} du_{0y}' = \frac{n_0}{2}\mathrm{erfc}\Big(\sqrt{\frac{1}{T_0'}}\Big) \tag{19}$$

We relate the dimensionless velocities at the free surface to those at the distance η using ballistic relations

$$u_{0x}' = u_x' - \frac{2\tan\alpha}{u_y' + \sqrt{u_y'^2+2}} \tag{20}$$

and

$$u_{0y}' = \sqrt{u_y'^2+2}. \tag{21}$$

We then carry out the change of variables in Eqs. 17 and 18 and normalize the result to find

$$\mathcal{M}(\eta) = \frac{n}{(2\pi T_0')^{3/2}} \exp[-\frac{1}{T_0'}] \frac{1}{\mathrm{erfc}(1/\sqrt{T_0'})} \times$$

$$\exp\Big[-\frac{u_x'^2}{2T_0'}\Big] \exp\Big[+\frac{(2\tan\alpha/T_0')u_x'}{u_y' + \sqrt{u_y'^2+2}}\Big] \times$$

$$\frac{|u_y'|}{\sqrt{u_y'^2+2}} \exp\Big[-\frac{2\tan^2\alpha/T_0'}{(u_y' + \sqrt{u_y'^2+2})^2}\Big] \times$$

$$\exp\Big[-\frac{u_y'^2}{2T_0'}\Big] \exp\Big[-\frac{u_z'^2}{2T_0'}\Big]. \tag{22}$$

From the first moment of this distribution, we calculate the mean velocity in the x-direction at $y = \eta$,

$$\frac{< u_x >}{\sqrt{T_0}} = \sqrt{\frac{2}{\pi}}\tan\alpha \frac{\exp[-g\eta\cos\alpha/T_0]}{\mathrm{erfc}\Big(\sqrt{g\eta\cos\alpha/T_0}\Big)}, \tag{23}$$

to which we add the mean velocity u_{0x} of the free surface that we omitted from Eq. 17. Although the corresponding momentum per unit volume decreases as $\exp[-g\eta\cos\alpha/T_0]$ from the free surface, Eq. 23 predicts a slight increase in the mean velocity. We plot the corresponding predictions for ν and u_x in the ballistic layer in Fig. 1 using $T_0/gd \sim 4.5$ (Fig 4) and $\nu_0 \sim 0.08$ (Fig. 1) from simulations. Despite inevitable discontinuities at the free surface, both predictions agree reasonably well with data, although it is unclear whether the actual velocity remains constant or increases slightly with η as this model predicts.

5 CONCLUSIONS

We have begun to refine the momentum balance of the "Super Stable Heap" of Taberlet et al. (2003). In doing so, we pointed out the exponential form of the volume fraction profile in the depth, and related its characteristic length to that of the velocity profile. We also proposed a simple model for the ballistic layer above the flow. It remains to explain why the volume fraction exhibits this behavior, to check the predictions of Eqs. 13 and 16 with additional simulations, and to predict profiles of velocity and temperature in terms of particle properties.

Acknowledgements. This work was supported by NASA grant NAG3-2705 and by US-France Cooperative Research grant NSF-INT-0233212.

REFERENCES

Jenkins, J. & Hanes, D. 1993. The balance of momentum and energy at an interface between colliding and freely flying grains in a rapid granular flow. *Phys. Fluids A* 5: 781–783.

Komatsu, T., Inagaki, S., Nakagawa, N., & Nasuno, S. 2001. Creep motion in a granular pile exhibiting steady surface flow. *Phys. Rev. Lett. 86*(9): 1757–1760.

Louge, M. 2003. Model for dense granular flows down bumpy inclines. *Phys. Rev. E* 67: 061303.

Pouliquen, O. 1999. Scaling laws in granular flows down rough inclined planes. *Phys. Fluids* 11: 542–548.

Silbert, L., Ertaş, D., Grest, G., Halsey, T., Levine, D., & Plimpton, S. 2001. Granular flow down an inclined plane: Bagnold scaling and rheology. *Phys. Rev. E* 64: 051302.

Taberlet, N., Richard, P., Delannay, R., & Louge, M. 2005, July. How sidewalls influence granular flows. In H.Herrmann, G. Gudehus, S. Luding, & K. Sommer (eds), *Powders and Grains 2005*: Stuttgart, Germany. AEMMG: A.A. Balkema.

Taberlet, N., Richard, P., Valance, A., Losert, W., Pasini, J.-M., Jenkins, J. T., & Delannay, R. 2003. Superstable granular heap in a thin channel. *Phys. Rev. Lett. 91*(26): 264301.